Electronic Supplementary Material (ESI) for RSC Advances.

Supplementary Information

A novel hexahydroquinazolin-2-amine based fluorescence sensor for Cu^{2+} from isolongifolanone and its biological applications

Zhonglong Wang,[a] Jinlai Yang,[b] Yiqin Yang,[c] Hua Fang,[d] Xu Xu,[a,e] Jian Rui,[a] Fan Su,[a] Haijun Xu,[a,e] Shifa Wang*[ae]

Institute of Chemical Engineering, Nanjing Forestry University, Nanjing, Jiangsu 210037, People's Republic of China

Jiangsu Key Lab of Biomass-based green Fuels and Chemicals, Nanjing, Jiangsu 210037, People's Republic of China

*Corresponding author: Email: wangshifa65@163.com; Fax: +86-25-85427812

Table S1. Crystal data and structure refinement for compound **2c.**

Empirical formula	$C_{22}H_{28}N_4$
Formula weight	348.48
Crystal system	monoclinic
a [Å]	7.6253(3)
b [Å]	10.0149(4)
c [Å]	12.9039(5)
α [deg]	95.695(2)
β [deg]	93.482(2)
γ [deg]	97.522(2)
Volume [$Å^3$]	969.41(7)
Z	2
D_c [g/cm^{-3}]	1.194
F (000)	376
T [K]	140(2)
Theta range for data collection [deg]	2.47 to 26.00
Wavelength [Å]	0.71073
Absorption coefficient [mm^{-1}]	0.072
Completeness to theta	26.00 (99.9 %)
Reflections collected/unique	24230 / 3808 [R(int) = 0.0940]
Data/restraints/parameters	3808 / 0 / 235
R_1, wR_2 [$I>2\sigma(I)$]	0.0692, 0.1510
R_1, wR_2 (all data)	0.1363, 0.1712
Goodness of fit on F^2	1.017
Largest diff. peak and hole [$e.Å^{-3}$]	0.771 and -0.223

Table S2. Comparison with other reported Cu^{2+} fluorescence probes

Probes	Detection limit (M)	Type(E/Q)	Bio- imaging	Selectivity	Reference
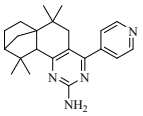	4.0×10^{-8}	Quenched	Blank mice (in vivo)	Cu^{2+}	this work
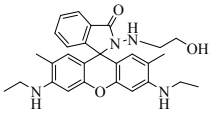	1.8×10^{-6}	Enhanced	MG63 cells (in vitro)	Cu^{2+}	[39]
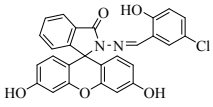	2.5×10^{-5}	Quenched	No data	Cu^{2+}	[40]
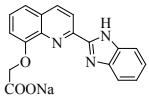	1.7×10^{-7}	Quenched	SMMC-7721 cells (in vitro)	Cu^{2+}, S^{2-}	[41]
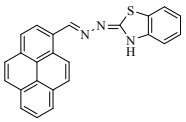	2.73×10^{-6}	Enhanced	RAW 264.7 cells (in vitro)	Cu^{2+}	[42]
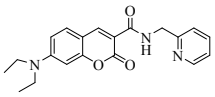	5×10^{-7}	Quenched	LLC-MK2 cells (in vitro)	Cu^{2+}	[43]
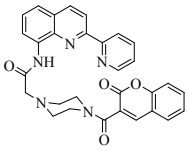	4.6×10^{-7}	Quenched	No data	Cu^{2+}	[44]
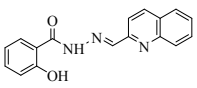	8.68×10^{-6}	Quenched	No data	Cu^{2+}	[45]
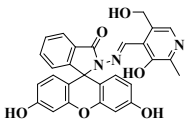	1.4×10^{-7}	Quenched	HepG2 cells (in vitro)	Cu^{2+}, Zn^{2+}	[46]

Supplemental Figures

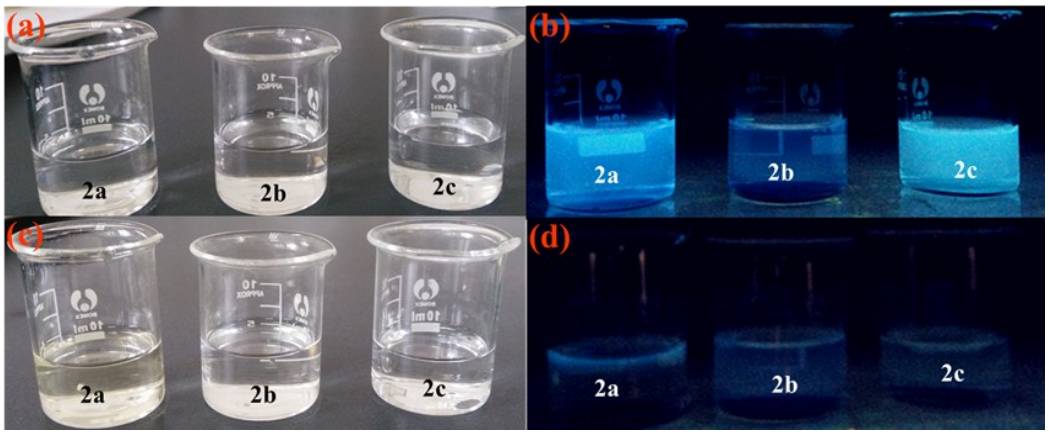

Fig. S1. Photographs of compounds **2a-2c** (1×10^{-4} M) in CH_3CH_2OH-H_2O (v/v=8/2) under sunlight (a) and 365 nm UV light (b); Photographs of compounds **2a-2c** (1×10^{-4} M) in presence of Cu^{2+} ion (1.5×10^{-3} M) in CH_3CH_2OH-H_2O (v/v=8/2) under sunlight (c) and 365 nm UV light (d).

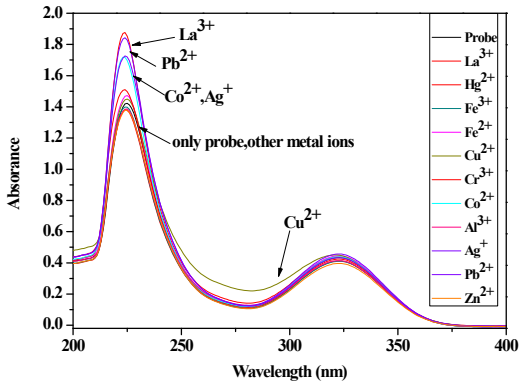

Fig. S2. UV-*vis* spectral changes of compound **2c** (1×10^{-4} M) upon addition of various metal ions (1×10^{-3} M) in CH_3CH_2OH-H_2O (v/v=8/2, 20mM HEPES buffer, pH=7.2) solution.

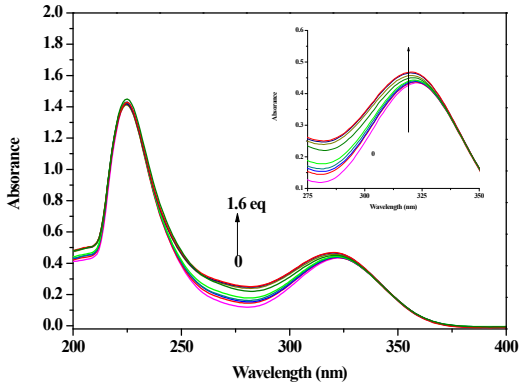

Fig. S3. UV-*vis* spectral changes of compound **2c** (1×10^{-4} M) with an increasing amount of Cu^{2+} ion in CH_3CH_2OH-H_2O (v/v=8/2, 20mM HEPES buffer, pH=7.2) solution.

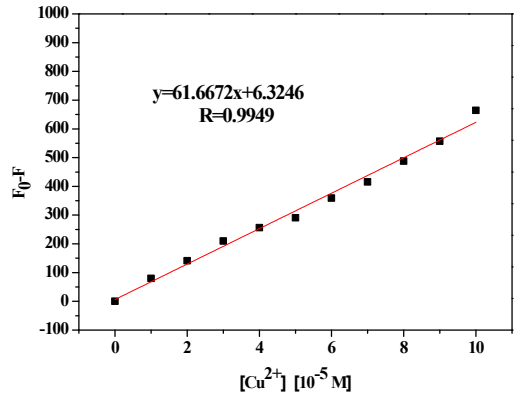

Fig. S4. Fluorescence intensity reduction of compound **2c** before and after quenching versus Cu^{2+} concentration. Excitation wavelength at 325 nm; Em. Slit at 12 nm; Ex. Slit at 5 nm.

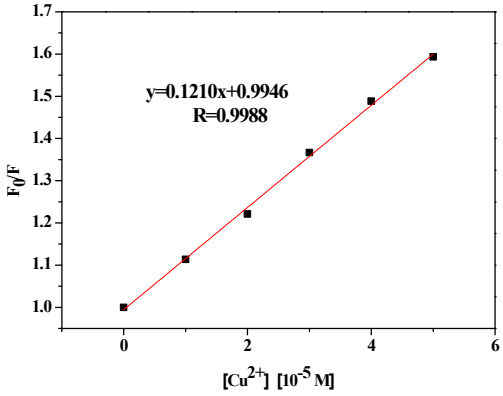

Fig. S5. The Stern-Volmer plots of compound **2c** with Cu^{2+} ion. Excitation wavelength at 325 nm; Em. Slit at 12 nm; Ex. Slit at 5 nm.

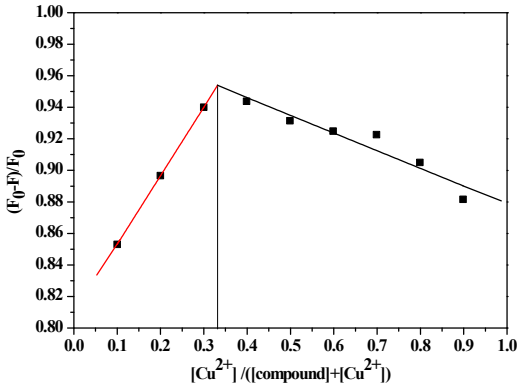

Fig. S6. Job plot of compound **2c** and Cu^{2+} in 8/2, v/v, 20 mM HEPES CH_3CH_2OH-H_2O, pH=7.2 (F_0 indicate fluorescence intensity of 10μM compound **2c**). The total concentrations of compound **2c** and Cu^{2+} were 1×10^{-5} M. Excitation wavelength at 325 nm; Em. Slit at 12 nm; Ex. Slit at 5 nm.

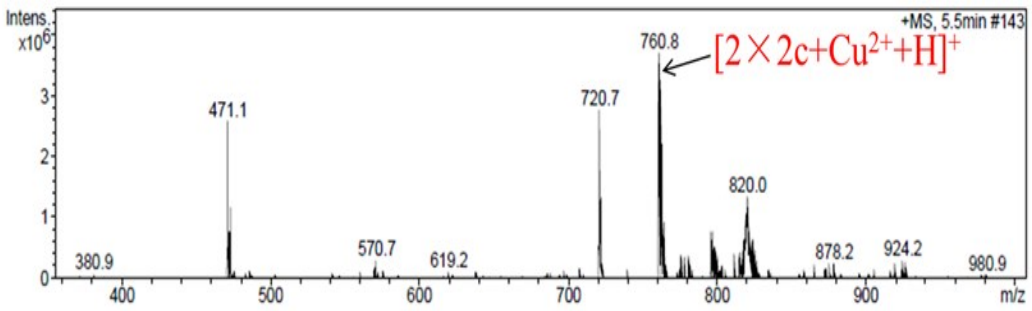

Fig. S7. Mass spectrometry of compound **2c** with Cu^{2+} measured by LC-MS.

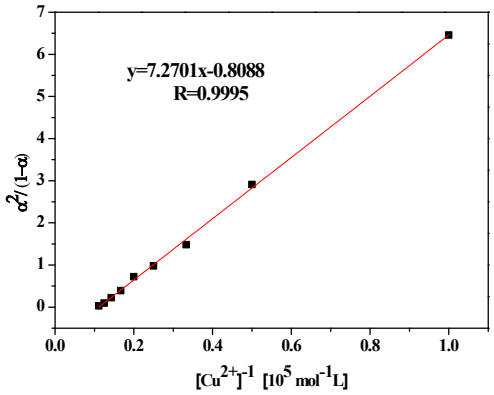

Fig. S8. The Benesi-Hildebrand plots of compound **2c** with Cu^{2+} ion. Excitation wavelength at 325 nm; Em. Slit at 12 nm; Ex. Slit at 5 nm.

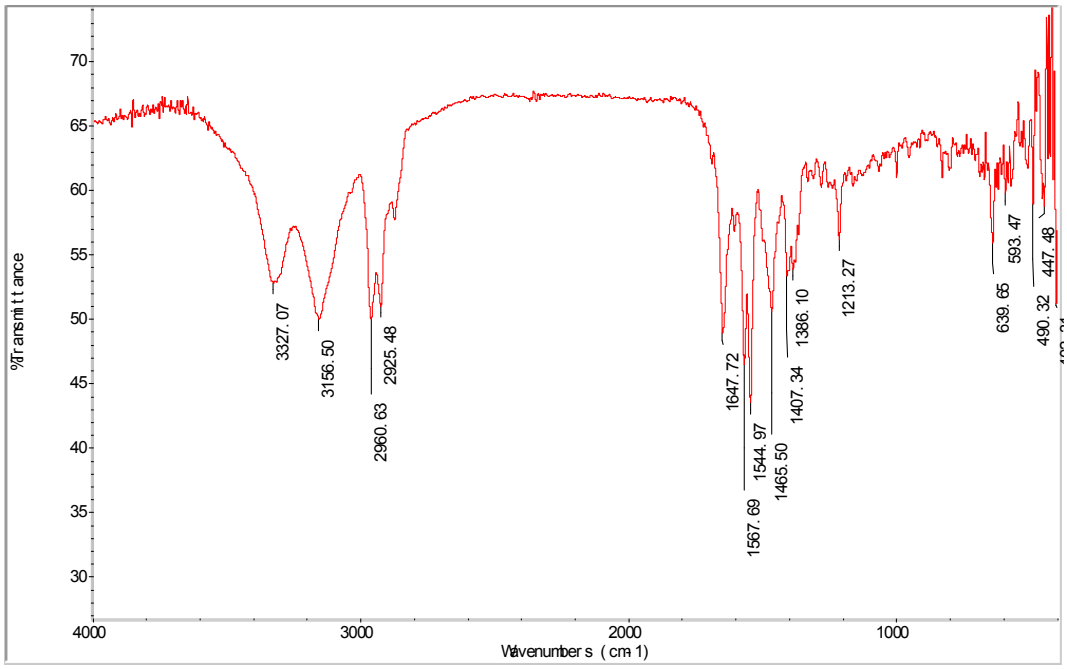

Fig. S9. The infrared spectra (KBr) of compound **2c**.

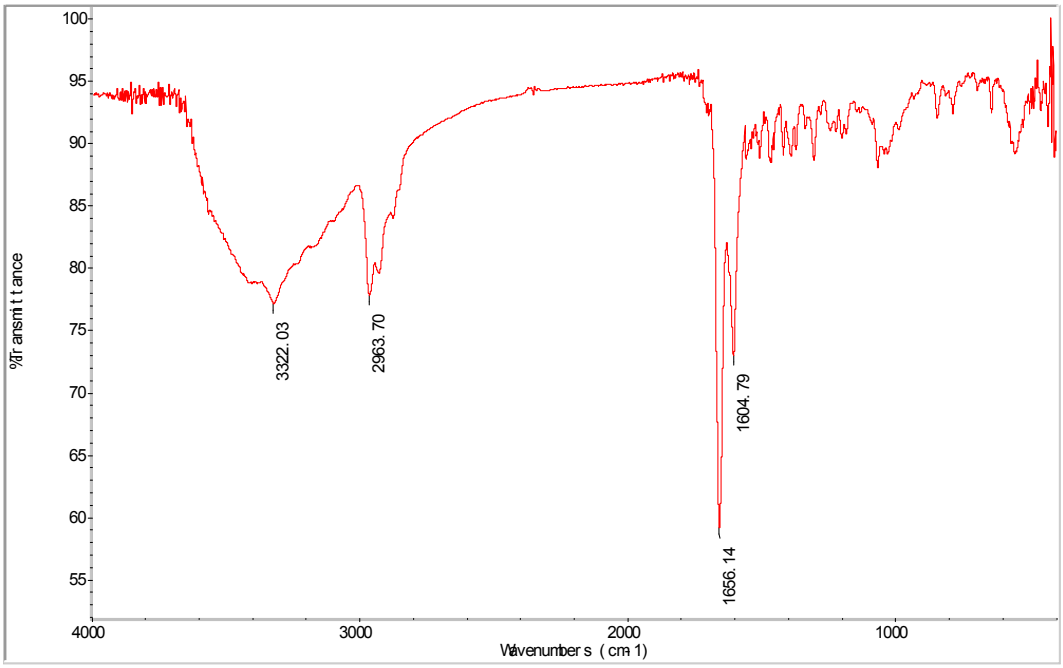

Fig. S10. The infrared spectra (KBr) of compound **2c** with Cu^{2+}.

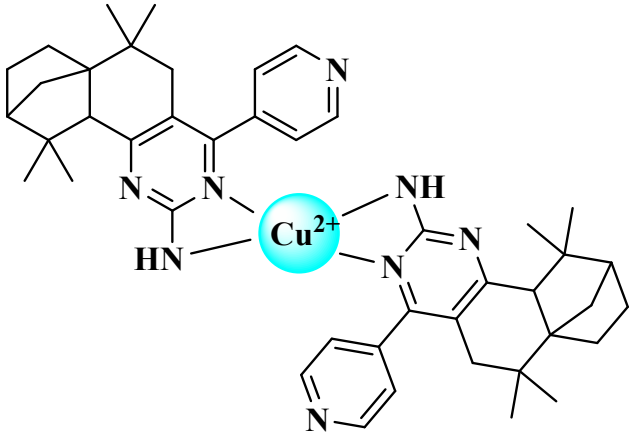

Fig. S11. The optimized binding mode of compound **2c** with Cu^{2+}.

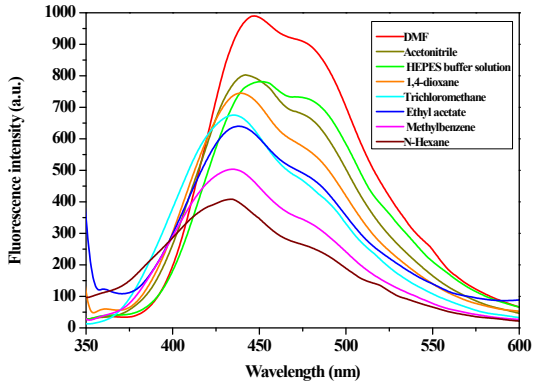

Fig. S12. Fluorescence spectra of compound **2c** (1×10^{-5} M) in different solvents. Excitation wavelength at 325 nm; Em. Slit at 12 nm; Ex. Slit at 5 nm.

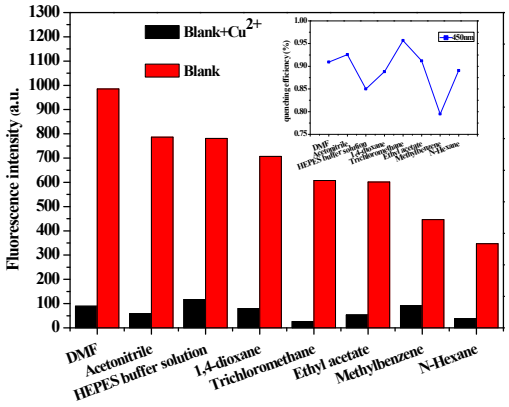

Fig. S13. Fluorescence intensity changes of compound **2c** (1×10^{-5} M) in absence and presence of Cu^{2+} (1×10^{-4} M) at 450nm in different solvents. Excitation wavelength at 325 nm; Em. Slit at 12 nm; Ex. Slit at 5 nm.

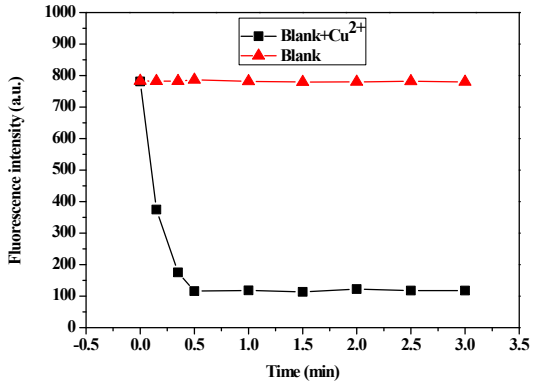

Fig. S14. The response time profiles of compound **2c** (1×10^{-5} M) towards Cu^{2+} ion (1×10^{-4} M) in CH_3CH_2OH-H_2O (v/v=8/2, 20mM HEPES buffer, pH=7.2) solution. Excitation wavelength at 325 nm; Em. Slit at 12 nm; Ex. Slit at 5 nm.

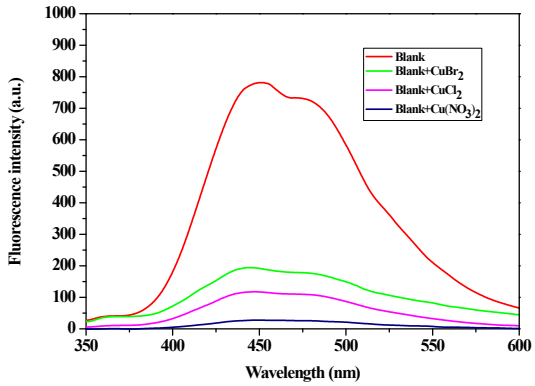

Fig. S15. Fluorescence spectra of compound **2c** (1×10^{-5} M) in CH_3CH_2OH-H_2O (v/v=8/2, 20mM HEPES buffer, pH=7.2) solution upon addition of various copper salts (1×10^{-4}M). Excitation wavelength at 325 nm; Em. Slit at 12 nm; Ex. Slit at 5 nm.

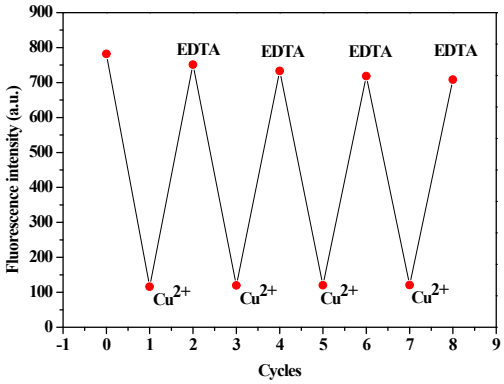

Fig. S16. Fluorescence intensity of compound **2c** (1×10^{-5} M) with Cu^{2+} ion (1×10^{-4} M) in presence of EDTA disodium (0-10 μM) in CH_3CH_2OH-H_2O (v/v=8/2, 20mM HEPES buffer, pH=7.2) solution. Excitation wavelength at 325 nm; Em. Slit at 12 nm; Ex. Slit at 5 nm.

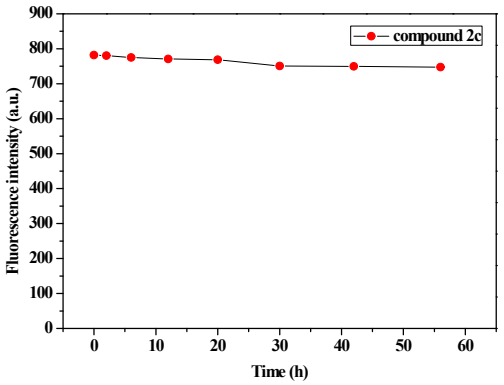

Fig. S17. Fluorescence intensity of compound **2c** in CH_3CH_2OH-H_2O (v/v=8/2, 20mM HEPES buffer, pH=7.2) solution under continuous illumination fluorescent lamp. Excitation wavelength at 325 nm; Em. Slit at 12 nm; Ex. Slit at 5 nm.

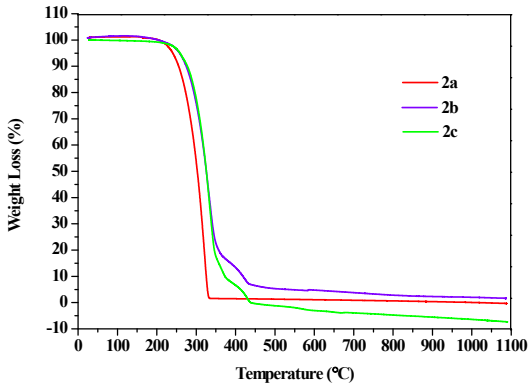

Fig. S18. TGA curves of compounds **2a-2c.**

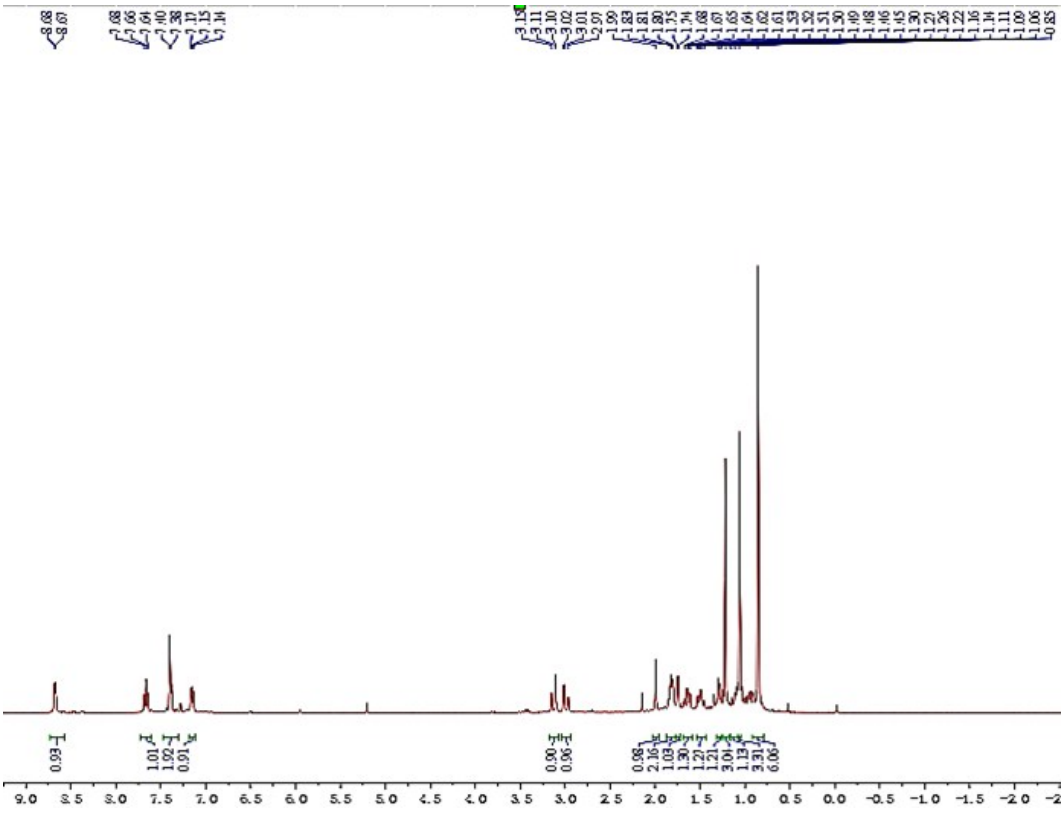

Fig. S19. ^{1}H NMR spectra of compound **1a** in $CDCl_3$.

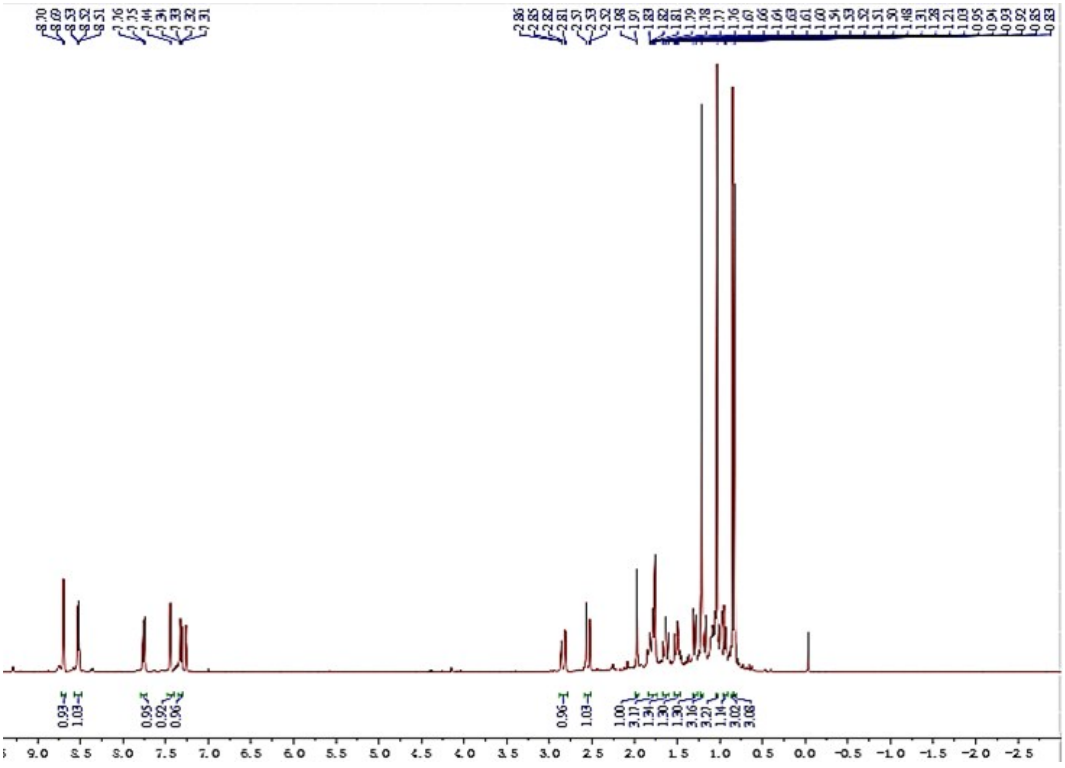

Fig. S20. ^{1}H NMR spectra of compound **1b** in $CDCl_3$.

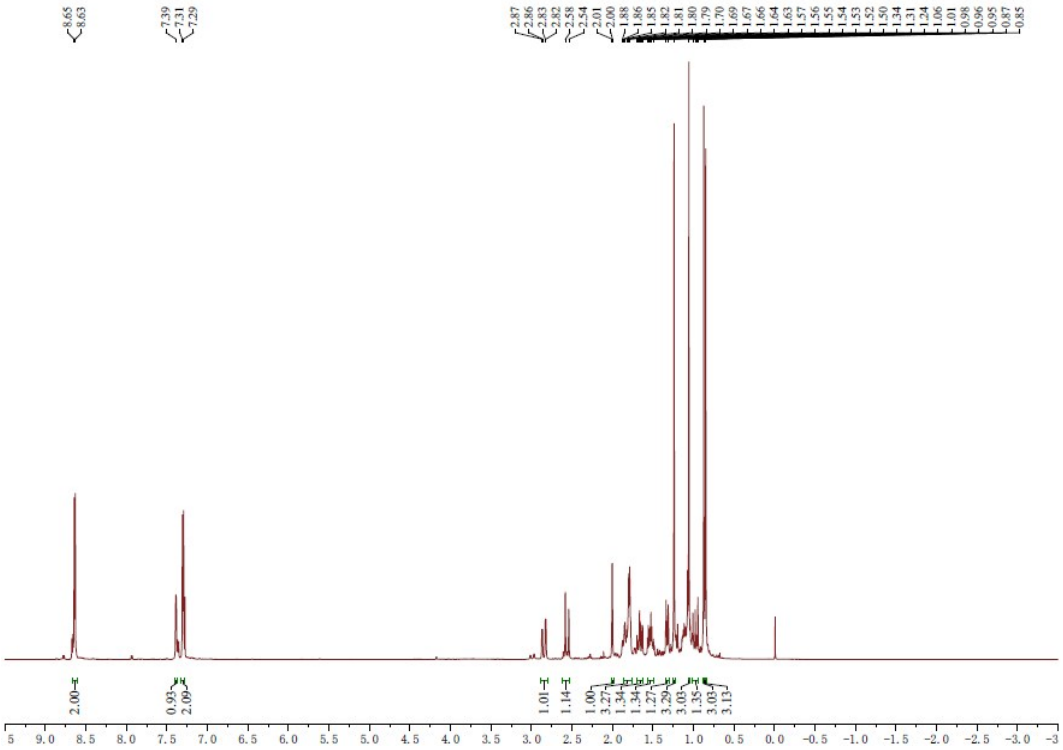

Fig. S21. ^{1}H NMR spectra of compound **1c** in $CDCl_3$.

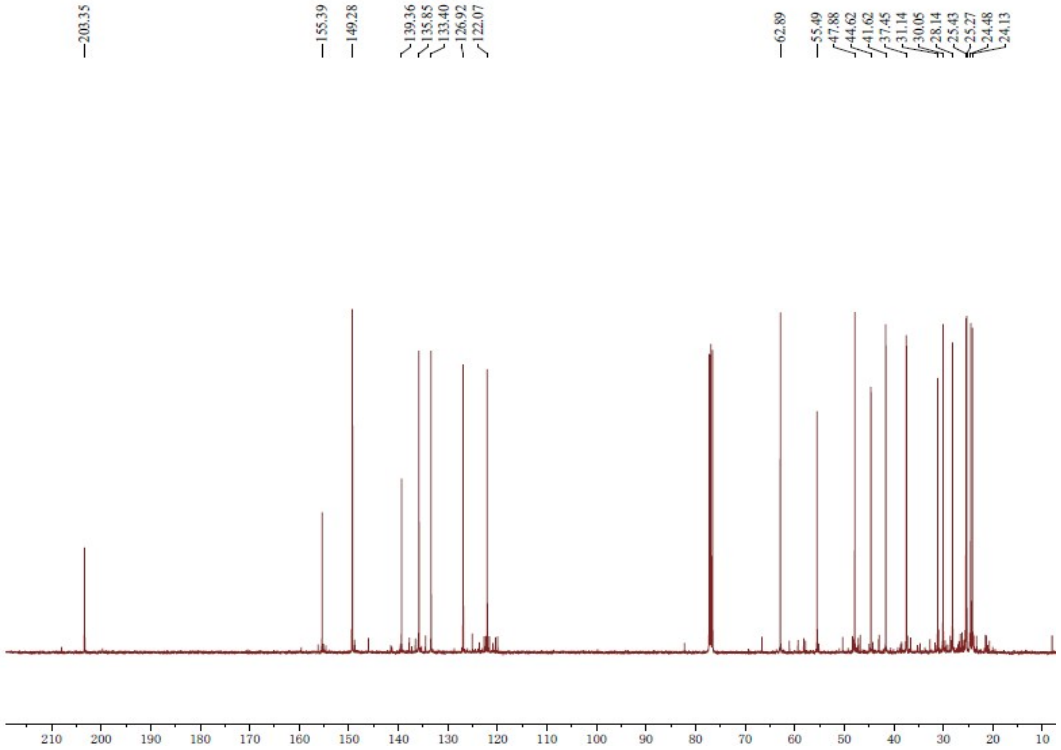

Fig. S22. ^{13}C NMR spectra of compound **1a** in $CDCl_3$.

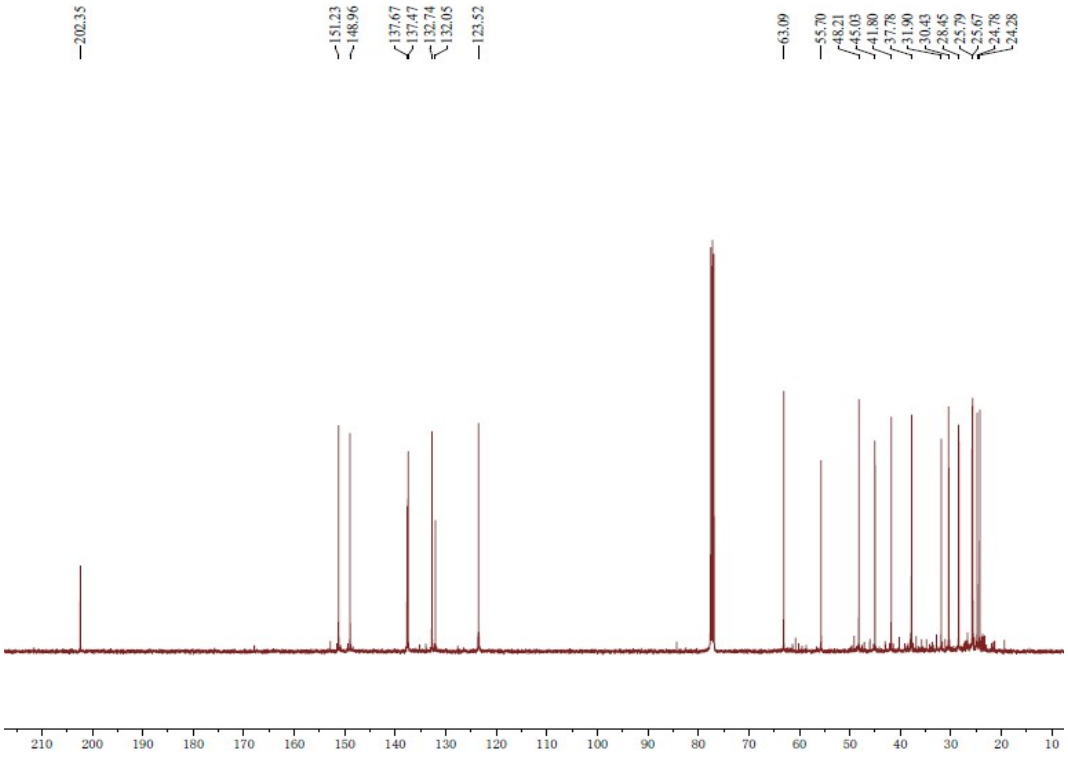

Fig. S23. ^{13}C NMR spectra of compound **1b** in $CDCl_3$.

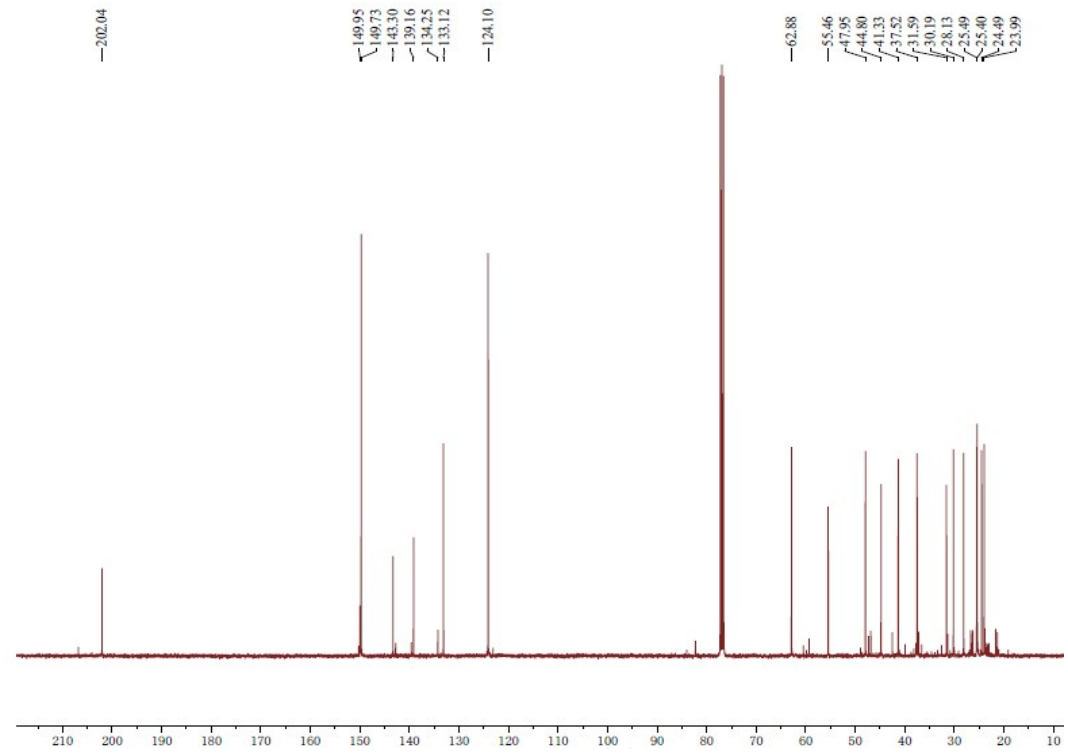

Fig. S24. ^{13}C NMR spectra of compound **1c** in $CDCl_3$.

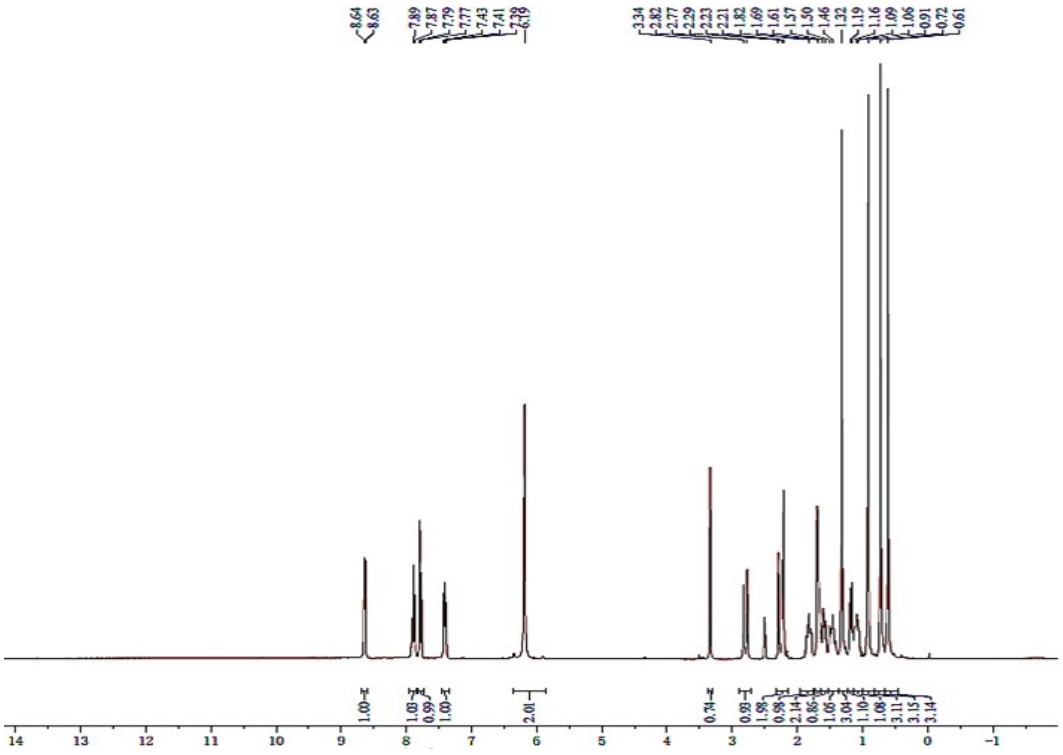

Fig. S25. ^{1}H NMR spectra of compound **2a** in DMSO-d_6.

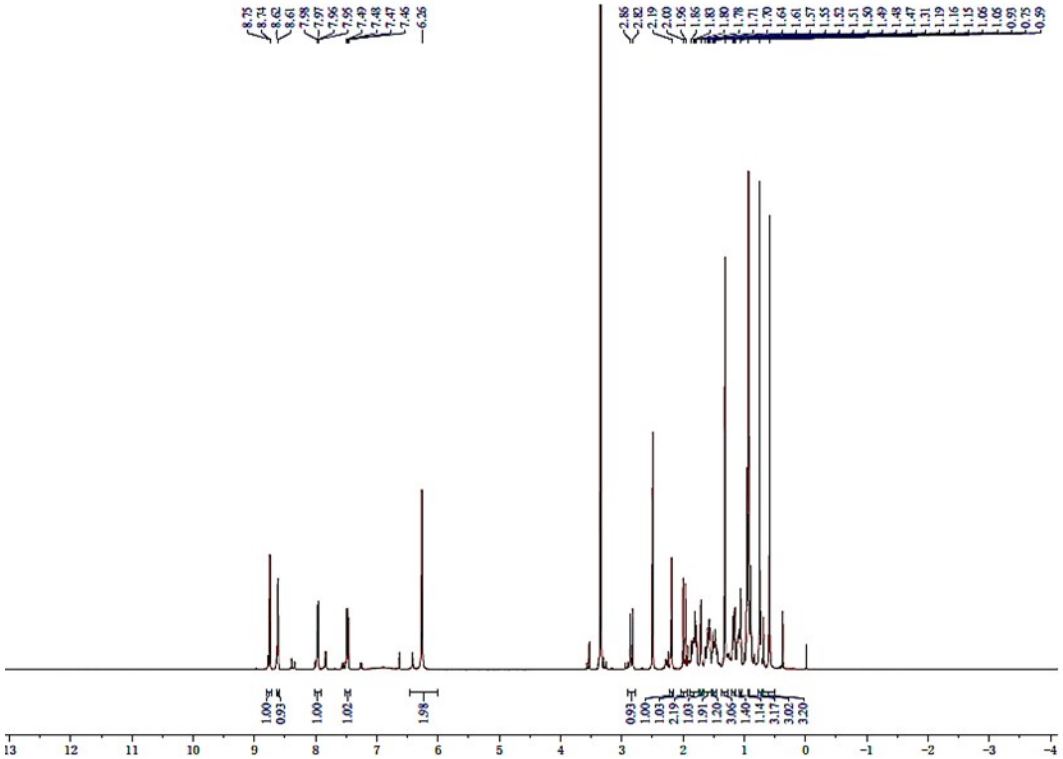

Fig. S26. ^{1}H NMR spectra of compound **2b** DMSO-d_6.

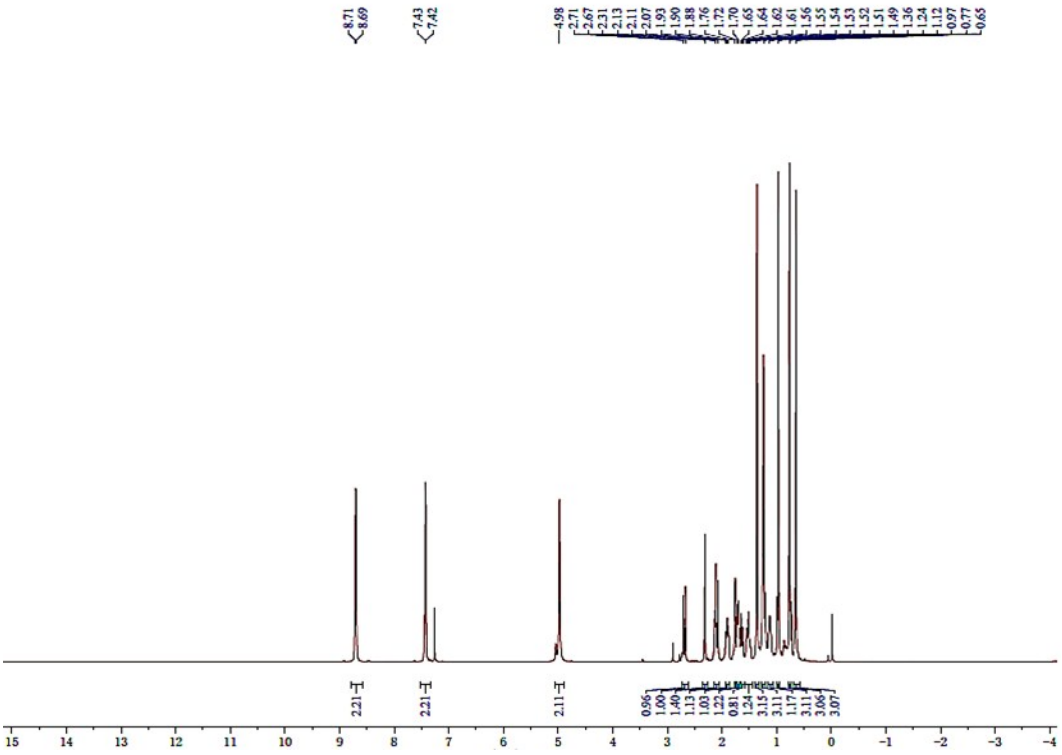

Fig. S27. ^{1}H NMR spectra of compound **2c** in $CDCl_3$.

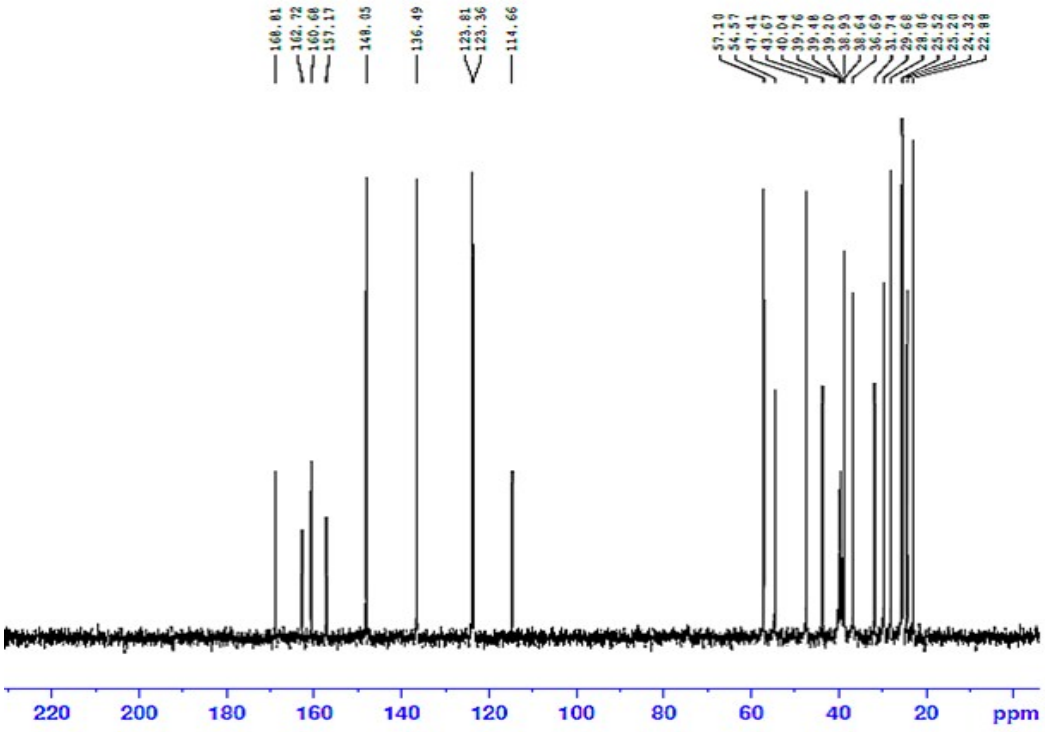

Fig. S28. ^{13}C NMR spectra of compound **2a** in DMSO-d_6.

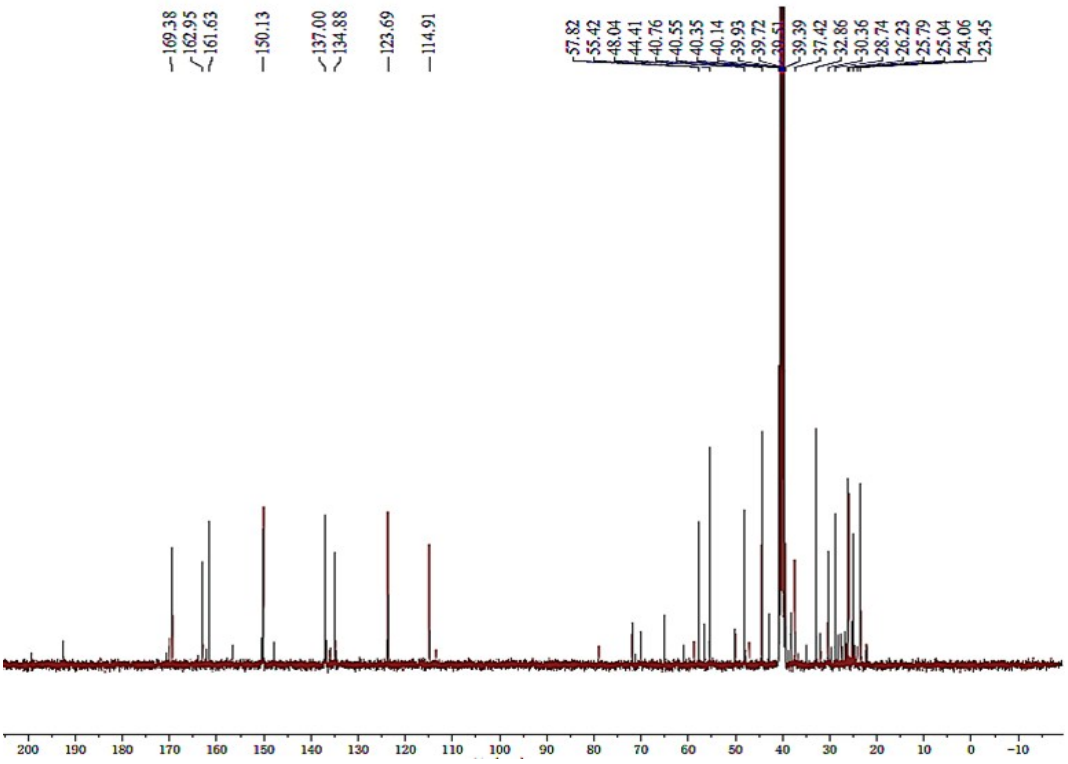

Fig. S29. ^{13}C NMR spectra of compound **2b** in DMSO-d_6.

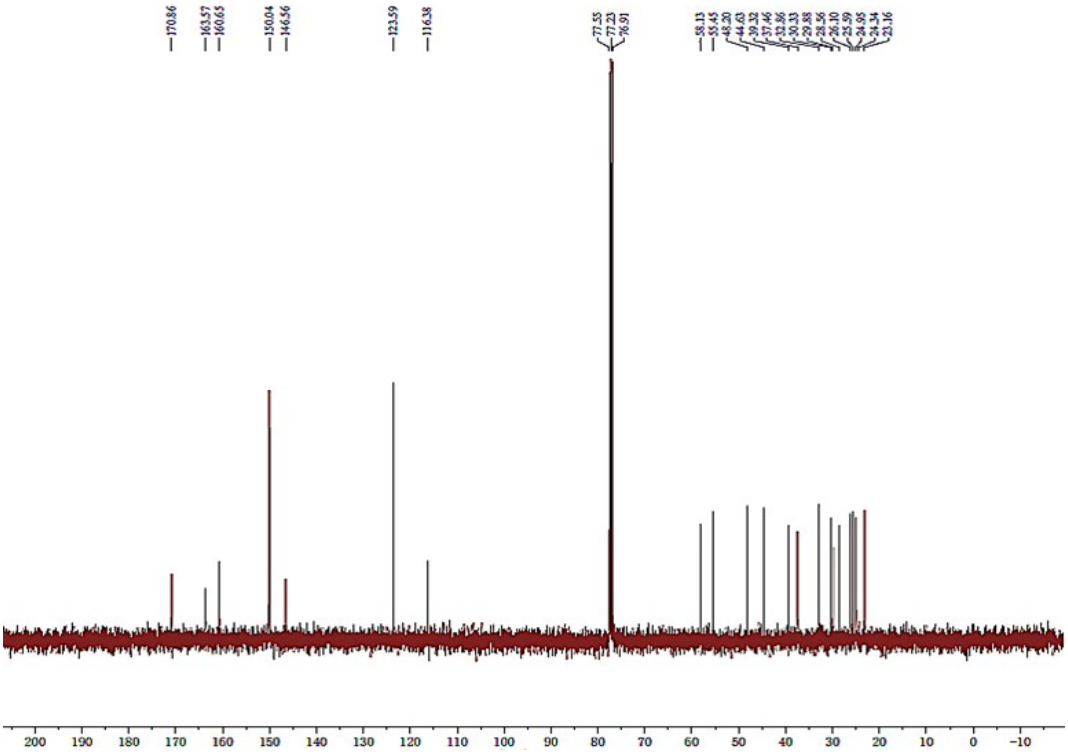

Fig. S30. ^{13}C NMR spectra of compound **2c** in $CDCl_3$

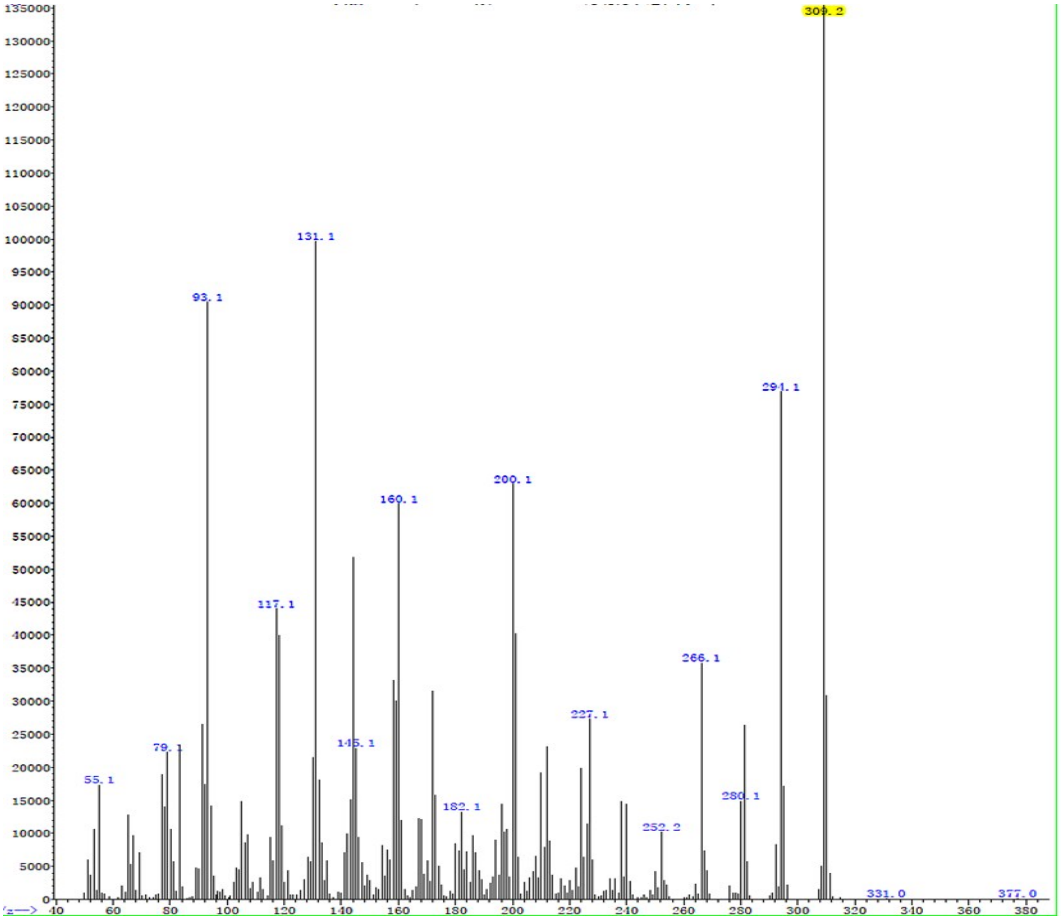

Fig. S31. Mass spectrometry of compound **1a**.

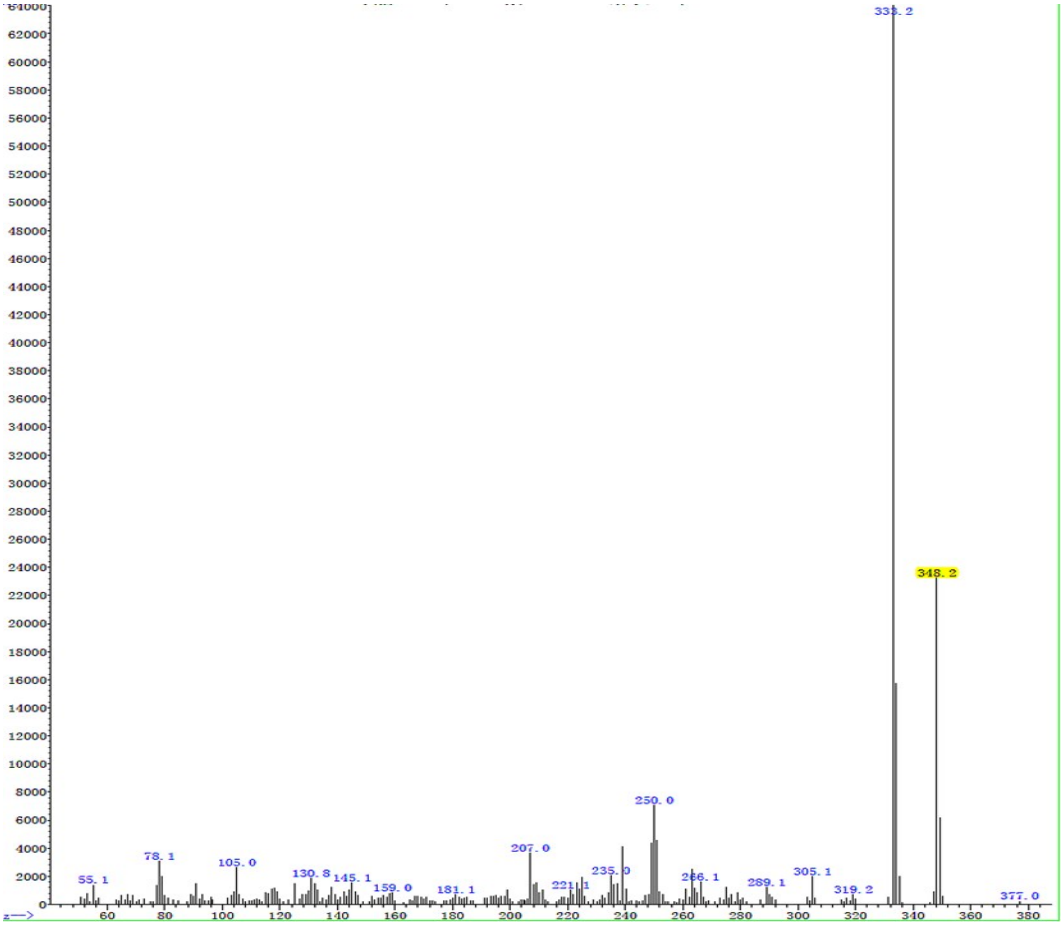

Fig. S32. Mass spectrometry of compound **2a**.

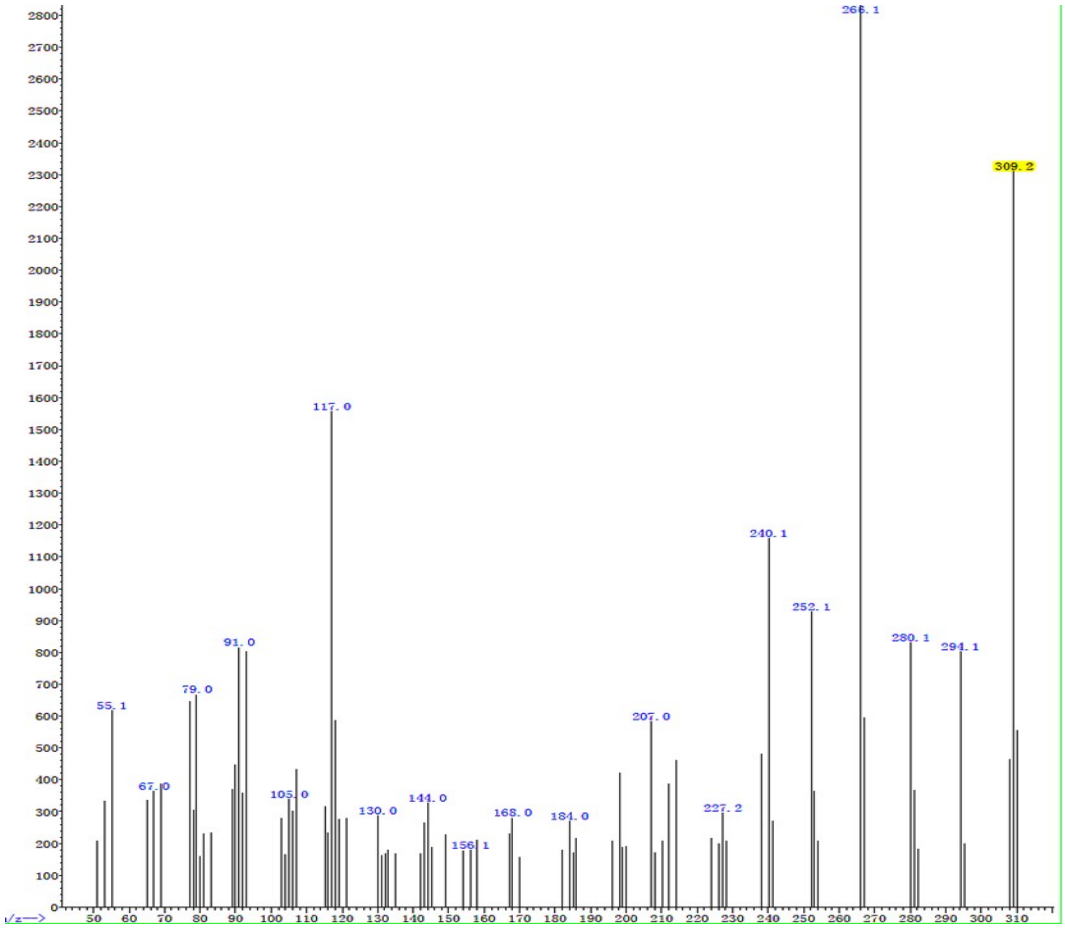

Fig. S33. Mass spectrometry of compound **1b**.

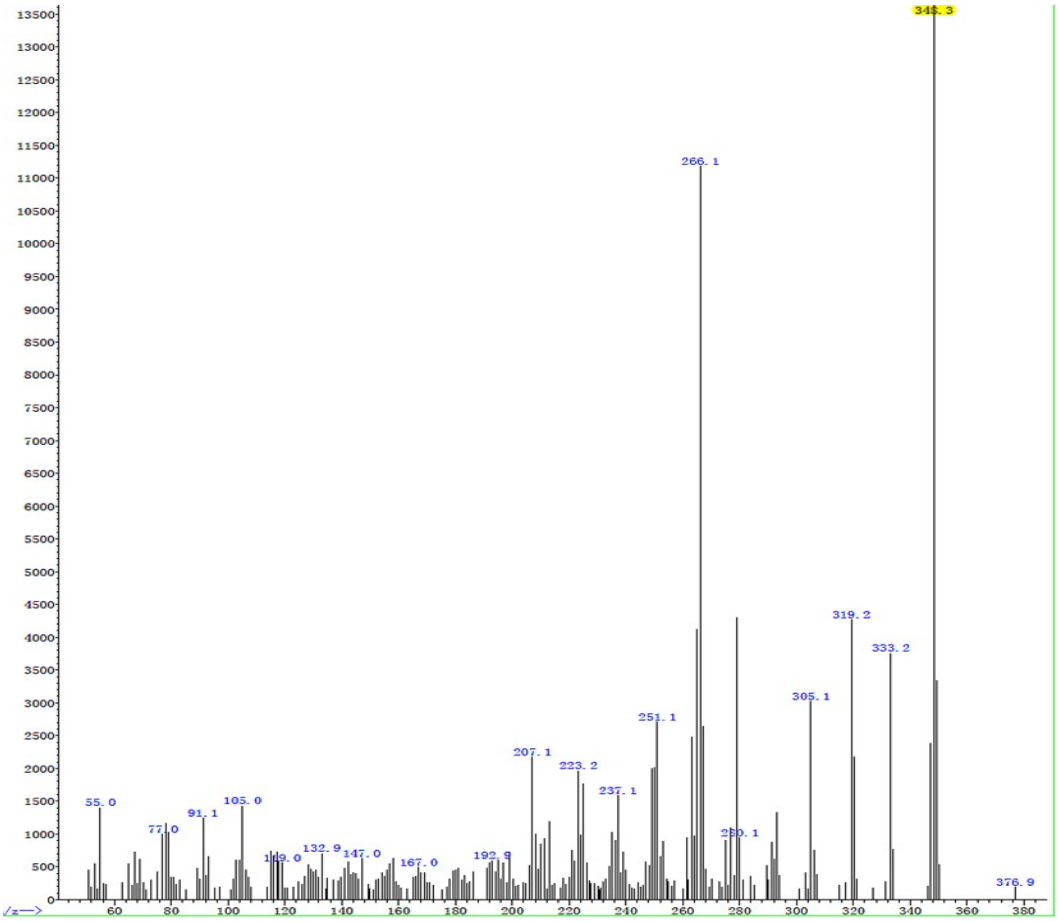

Fig. S34. Mass spectrometry of compound **2b**.

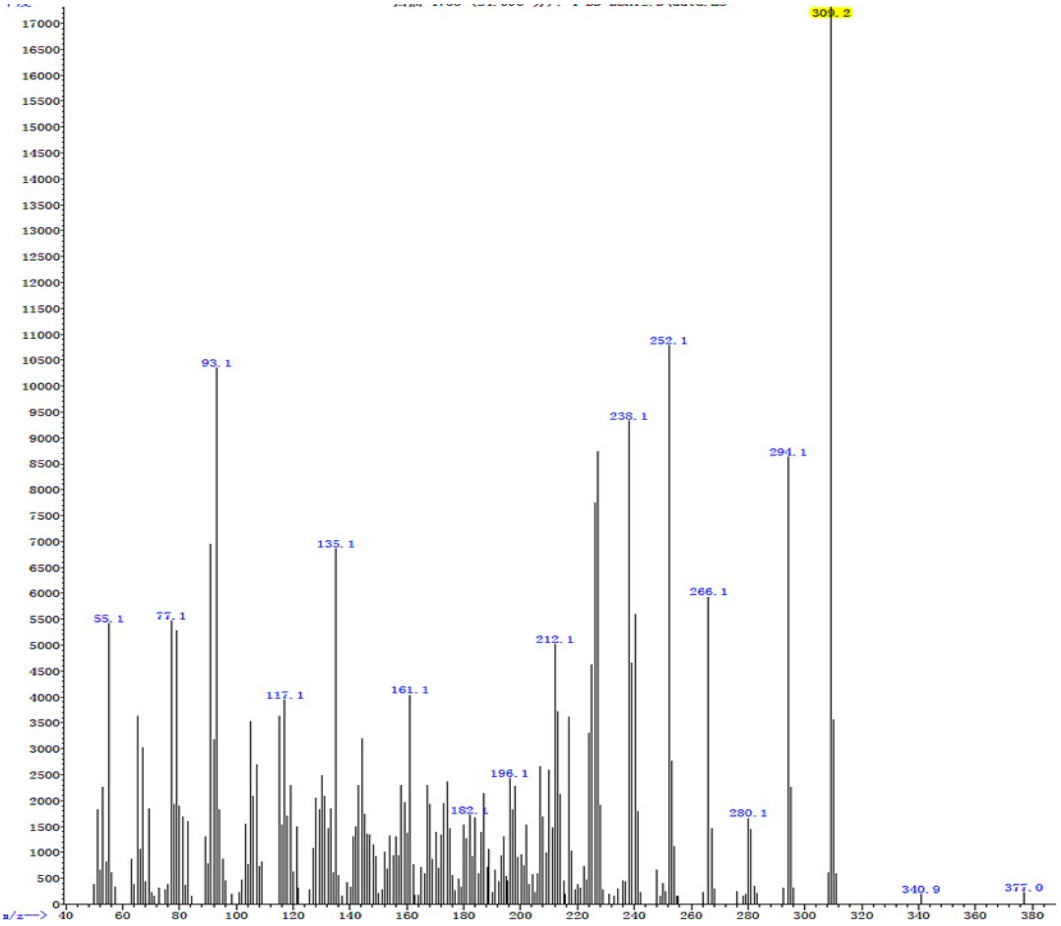

Fig. S35. Mass spectrometry of compound **1c**.

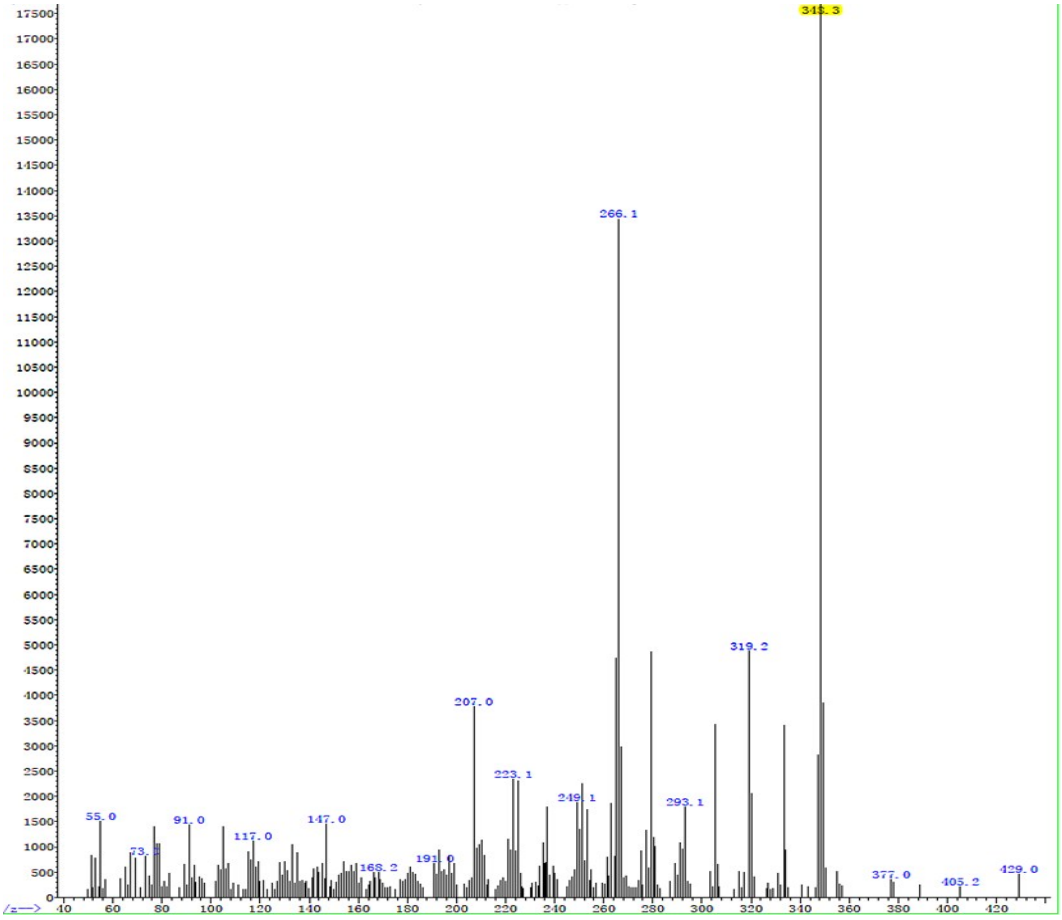

Fig. S36. Mass spectrometry of compound **2c**.

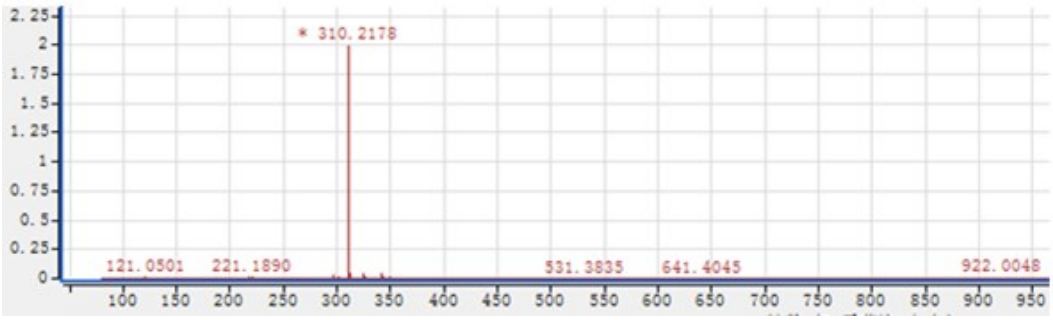

Fig. S37. HRMS of compound **1a**.

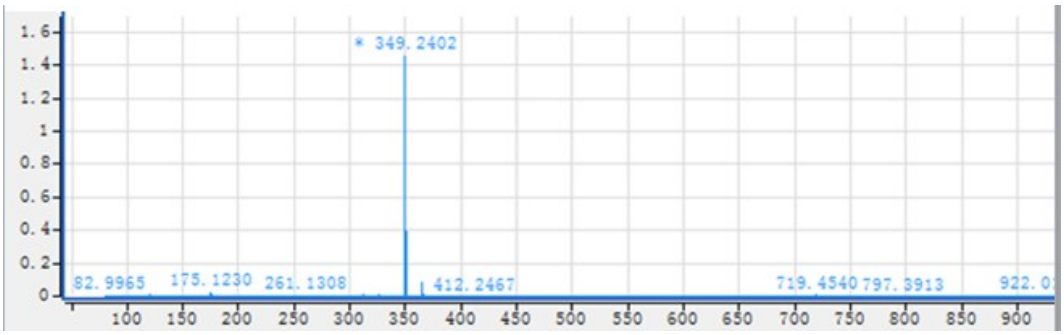

Fig. S38. HRMS of compound **2a**.

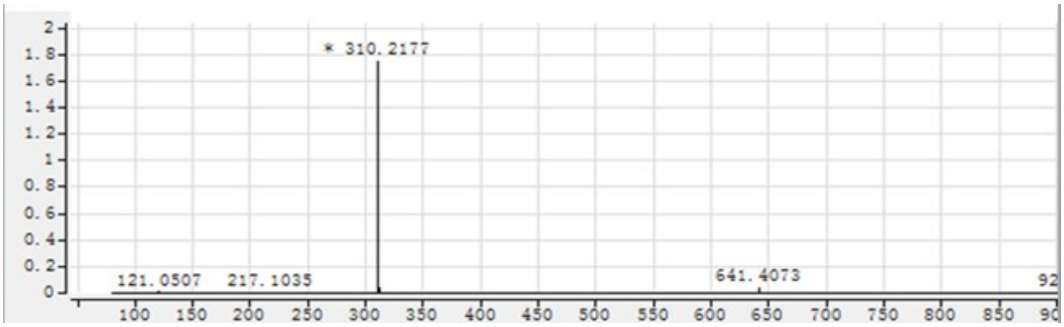

Fig. S39. HRMS of compound **1b**.

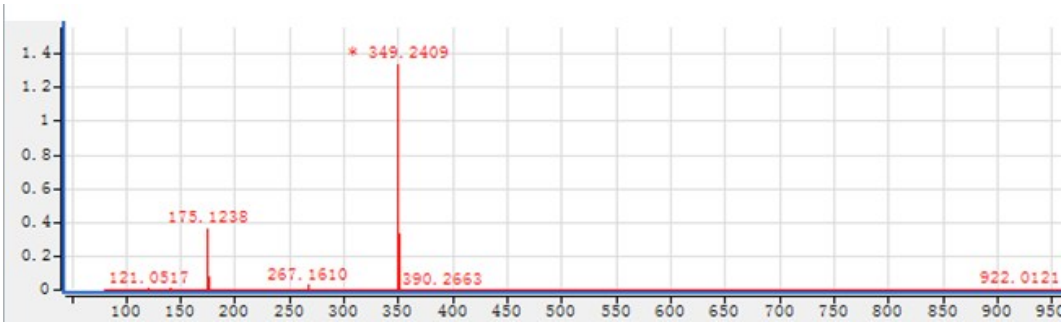

Fig. S40. HRMS of compound **2b**.

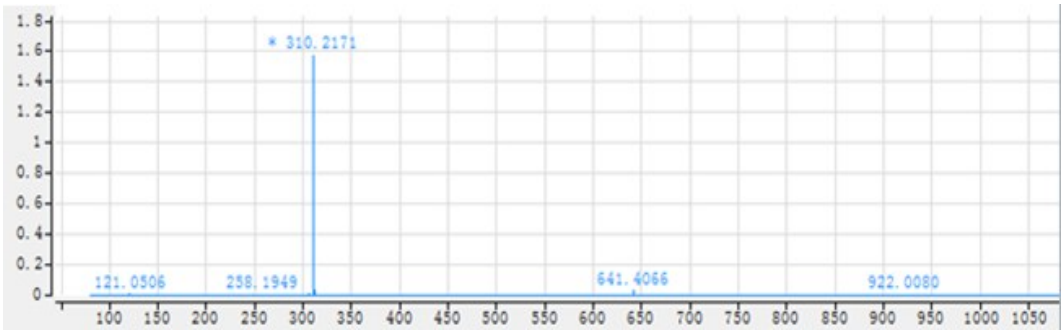

Fig. S41. HRMS of compound **1c**.

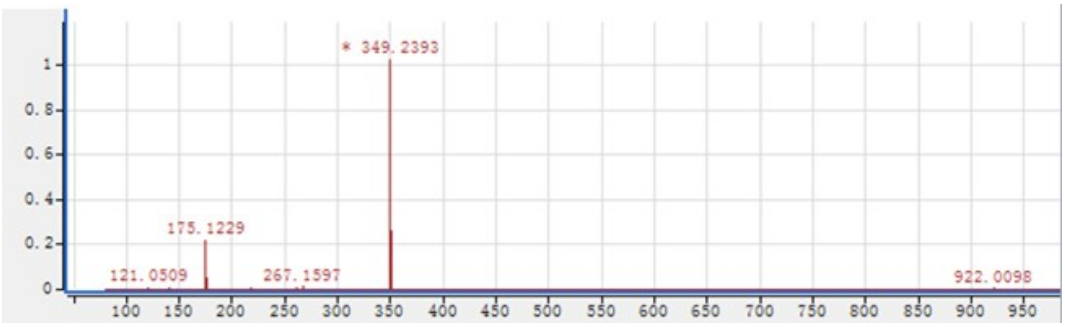

Fig. S42. HRMS of compound **2c**.

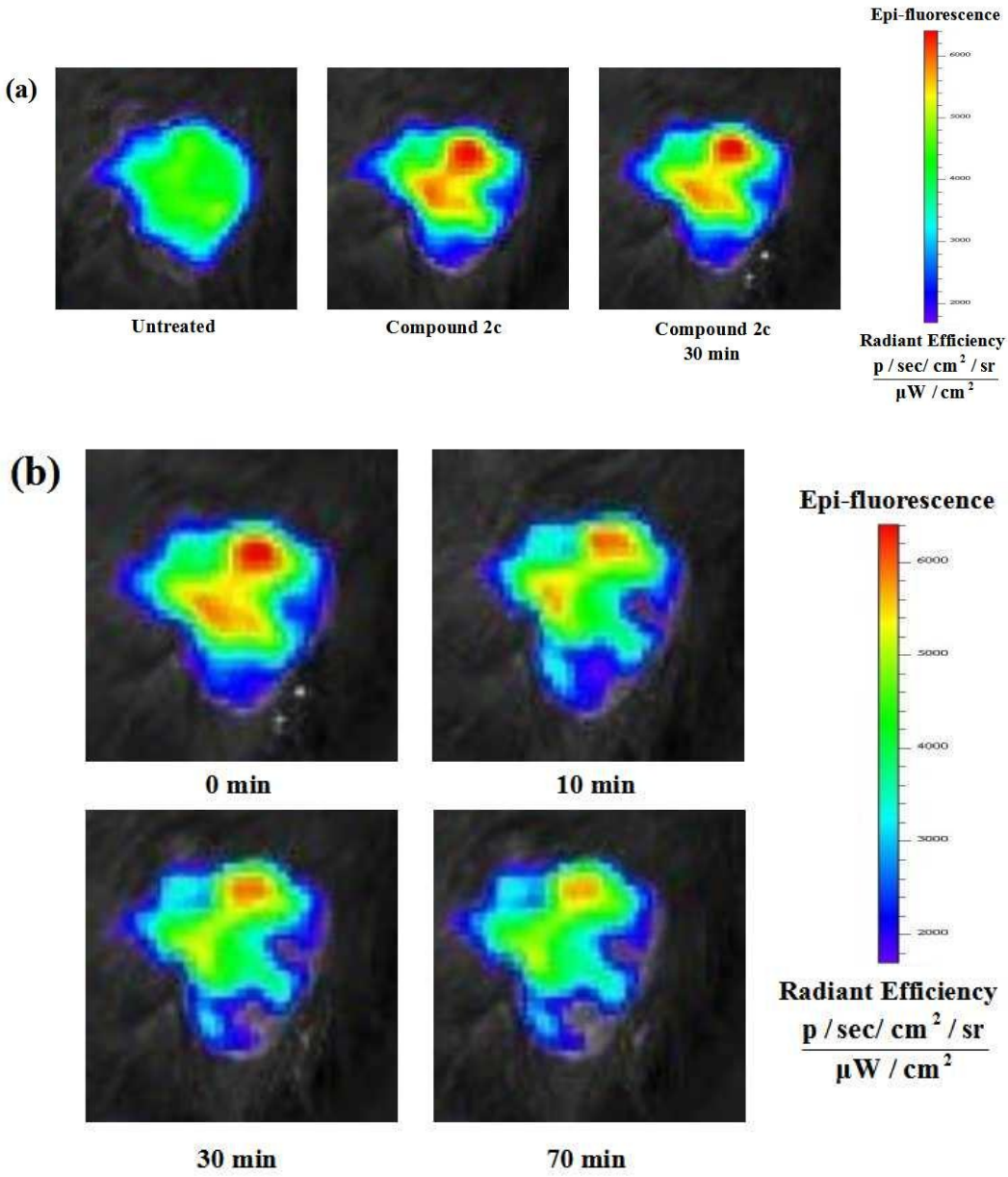

Fig. S43. (a) The zoomed in versions of injected part (the hip of mouse) in **Fig. 10a**, (b) the zoomed in versions of injected part (the hip of mouse) in **Fig. 10b**.